EUROGRAPHICS 2009 / P. Dutré and M. Stamminger
(Guest Editors)

Volume 28 (2009), Number 2

An Analytical Solution to Single Scattering in Homogeneous Participating Media

Vincent Pegoraro [1] Steven G. Parker [1,2]

[1]University of Utah [2]NVIDIA Corporation

Abstract

Despite their numerous applications, efficiently rendering participating media remains a challenging task due to the intricacy of the radiative transport equation. As they provide a generic means of solving a wide variety of problems, numerical methods are most often used to solve the air-light integral even under simplifying assumptions. In this paper, we present a novel analytical approach to single scattering from isotropic point light sources in homogeneous media. We derive the first closed-form solution to the air-light integral in isotropic media and extend this formulation to anisotropic phase functions. The technique relies neither on pre-computation nor on storage, and we provide a practical implementation allowing for an explicit control on the accuracy of the solutions. Finally, we demonstrate its quantitative and qualitative benefits over both previous numerical and analytical approaches.

Categories and Subject Descriptors (according to ACM CCS): I.3.7 [Computer Graphics]: Three-Dimensional Graphics and Realism—Color, shading, shadowing, and texture

1. Introduction

Participating media model a wide variety of elements and the ability to faithfully reproduce their characteristics has many scientific applications. Although realistic rendering is often of concern to the movie and gaming industries, such interest also emerged among safety oriented research where typical scenarios entail predicting the visibility of traffic signs in a foggy weather or exit signs in a smoke-filled room.

However, efficiently simulating accurate light transport in such media remains a challenging task due to the intricacy of the equation governing radiative energy transfer. While Monte-Carlo and finite element techniques made complex problems tractable, generic numerical methods such as ray-marching and volume-slicing are most often used to compute a solution to the air-light integral even under simplifying assumptions. Although simple and practical, these techniques do not exploit the characteristics of the integrand of concern and are prompt to under-sampling artifacts.

Considering optically thin media lit by isotropic light sources, this paper presents an analytical approach to solving the single scattering air-light integral. It provides a novel reformulation of the latter as to yield a closed-form solution in terms of well-known functions for isotropic media, and extends the previous results to anisotropic phase functions.

This document starts by providing an overview of the related work and theoretical background on the air-light integral. The derivation of the analytical solutions as well as a practical implementation are then presented followed by both quantitative and qualitative results along with a discussion of the potential limitations of the method.

2. Related Work

Several techniques have been proposed in the computer graphics literature for rendering participating media, ranging from computationally expensive detailed simulations of multiple scattering in complex environments to drastic approximations primarily concerned with interactivity. A good survey of these methods is provided in [CPCP*05].

Optically thin media were first investigated by Blinn [Bli82] who introduced an analytical model for homogeneous media under the assumption of an infinitely distant light source and viewer. Later, Max [Max86] proposed to evaluate the air-light integral by fitting Hermite cubic polynomials on adaptively subdivided intervals along the ray.

Despite the conceptual simplicity of single scattering in a homogeneous medium, numerical methods provide a convenient means of dealing with the actual complexity of the corresponding integrand and many techniques based on ray-marching or volume-slicing have consequently been developed. Considering anisotropic media lit by spotlights of varying intensity, Nishita et al. [NMN87] proposed to bound each light by a cone as to restrict ray-marching to illuminated segments only. Dobashi et al. [DYN00] exploit the GPU capabilities to perform hardware blending of view-aligned slices mapped with textures describing the light intensity and computed on the CPU. To reduce aliasing without compromising interactivity, they [DYN02] subsequently proposed to approximate the integral of a product as a product of integrals, allowing the low frequencies to be coarsely evaluated on the CPU while higher-frequencies are finely sampled via textured subplanes. Being also concerned about the trade-offs between aliasing and cost, Imagire et al. [IJTN07] proposed to divide the space into a set of sampling hulls of which contributions are hardware-blended, allowing for higher sampling rates while limiting read-write memory accesses. In their paper [ET08], the authors also resort to ray-marching to compute the final scattering intensity of a pixel based on the number of lit samples, and build a min-max MIP-MAP of the shadow map to allow finer sampling in potentially high-frequency regions. Jittering of the initial samples along each ray is used to remove aliasing artifacts from regular sampling, alas introducing noise instead.

Besides the image post-processing technique of Mitchell [Mit07], several analytical approaches have also been proposed. Hoffman et al. [HP02] and Riley et al. [REK*04] derived such models for single atmospheric scattering of directional sun light in constant and exponentially decreasing medium densities respectively. Considering point light sources, Lecocq et al. [LMAK00] presented an angular formulation of the radiative transport equation and expand the resulting integrand into a Taylor series allowing each term to be analytically integrated. Biri et al. [BMA03, BAM06] subsequently combined this angular formulation with volumetric shadows by expressing the ray integral as a difference of contributions along each segment. While presenting theoretical advantages, the derivation of each term of the Taylor expansion however usually requires a human intervention and the method consequently does not lend itself to well-defined precision requirements. In their paper, Sun et al. [SRNN05] rederive Lecocq's formulation using a different notation and perform an additional linear change of variable to simplify it further. The integral is then tabulated via numerical precomputation and cheaply interpolated on the GPU during rendering, hence trading computation for storage. Also, while the angular coordinate of this 2D table is bounded, the second degree of freedom is a distance of which extent might not be known in advance. Wyman et al. [WR08] subsequently combined this approach with ray-marching as to handle light-shafts and anisotropic light sources.

3. An Analytical Solution to Single Scattering

This section starts by describing the mathematical formulation of the air-light integral in homogeneous participating media under the assumption of an isotropic light. An analytical solution for isotropic media is subsequently derived before extending this result to anisotropic phase functions.

3.1. The Air-Light Integral

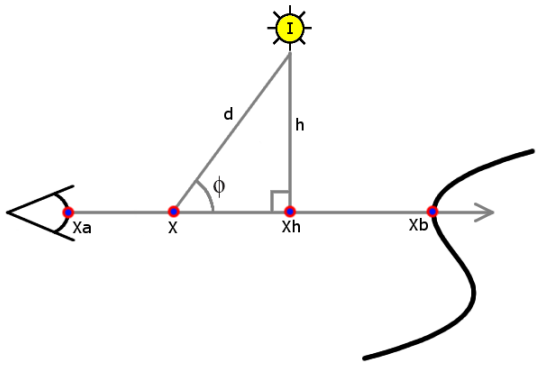

Figure 1: *Illustration of the terms involved in the computation of the air-light integral.*

For a given wavelength, the radiative transport equation (RTE) describes the change of radiance L along a ray of direction $\vec{\omega}$ through a medium as [SH81]

$$\frac{\partial L(x,\vec{\omega})}{\partial x} = \kappa_a(x)(L_e(x,\vec{\omega}) - L(x,\vec{\omega})) + \kappa_s(x)(L_i(x,\vec{\omega}) - L(x,\vec{\omega})), \quad (1)$$

where κ_a is the absorption coefficient, κ_s the scattering coefficient, L_e the emitted radiance, and L_i the in-scattered radiance. Defining the boundary condition as the background radiance L_b, the extinction coefficient as $\kappa_t = \kappa_a + \kappa_s$ and the optical thickness as $\tau(x_a, x_b) = \int_{x_a}^{x_b} \kappa_t(x)dx$, the RTE accepts an integral form which at a point x_a reads

$$L(x_a,\vec{\omega}) = e^{-\tau(x_a,x_b)}L_b(x_b,\vec{\omega}) + \int_{x_a}^{x_b} e^{-\tau(x_a,x)}(\kappa_a(x)L_e(x,\vec{\omega}) + \kappa_s(x)L_i(x,\vec{\omega}))dx. \quad (2)$$

Assuming a homogeneous non-emitting medium of phase function Φ illuminated by an isotropic point light source of intensity I, the in-scattered radiance reads [NMN87]

$$L_i(x,\vec{\omega}) = I\frac{e^{-\kappa_t d(x,\vec{\omega})}}{d(x,\vec{\omega})^2}\Phi(\phi(x,\vec{\omega})) = I\frac{e^{-\kappa_t\sqrt{h^2+(x-x_h)^2}}}{h^2+(x-x_h)^2}\Phi\left(\arctan\left(\frac{x-x_h}{h}\right)+\frac{\pi}{2}\right) \quad (3)$$

where h is the distance from the light to the given ray and x_h the coordinate of its projection onto it, both being constant

for a given orientation along the ray as illustrated in figure 1. Defining L_m as the medium radiance, equation 2 becomes

$$L(x_a,\vec{\omega}) = e^{-\kappa_t(x_b-x_a)}L_b(x_b,\vec{\omega}) + \underbrace{I\kappa_s e^{\kappa_t x_a}\int_{x_a}^{x_b}\frac{e^{-\kappa_t\left(x+\sqrt{h^2+(x-x_h)^2}\right)}}{h^2+(x-x_h)^2}\,\Phi\left(\arctan\left(\frac{x-x_h}{h}\right)+\frac{\pi}{2}\right)dx}_{L_m(x_a,x_b,\vec{\omega})}. \tag{4}$$

In this work, the impact of the medium on surface shading is assumed to be dominated by extinction phenomena and the background radiance is therefore computed as follows

$$L_b(x_b,\vec{\omega}) = I\frac{e^{-\kappa_t d(x_b,\vec{\omega})}}{d(x_b,\vec{\omega})^2}\beta(\vec{\omega},\vec{\omega}_i,\vec{n})\;\vec{\omega}_i\cdot\vec{n}, \tag{5}$$

where $\vec{n}$ is the surface normal at x_b, $\vec{\omega}_i$ is a vector directed towards the light source and β is the bidirectional reflectance distribution function (BRDF). The evaluation of the medium radiance is addressed in the remainder of this document.

3.2. Analytical Reformulation

We start by simplifying the formulation of the medium radiance such that the integrand becomes a function of only 2 parameters. For this, we make the following change of variable $u = \frac{x-x_h}{h}$, and define the optical distance from the light source to the ray as $H = \kappa_t h$, which yields

$$L_m(x_a,x_b,\vec{\omega}) = I\frac{\kappa_s}{h}e^{\kappa_t(x_a-x_h)}\int_{\frac{x_a-x_h}{h}}^{\frac{x_b-x_h}{h}}\frac{e^{-H(u+\sqrt{1+u^2})}}{1+u^2}\Phi\left(\arctan(u)+\frac{\pi}{2}\right)du. \tag{6}$$

We also note that almost all phase functions are expressed in terms of the cosine of the angle and define Φ_c such that $\Phi(\phi) = \Phi_c(\cos(\phi))$. Plugging this into equation 6 gives

$$L_m(x_a,x_b,\vec{\omega}) = I\frac{\kappa_s}{h}e^{\kappa_t(x_a-x_h)}\int_{\frac{x_a-x_h}{h}}^{\frac{x_b-x_h}{h}}\frac{e^{-H(u+\sqrt{1+u^2})}}{1+u^2}\Phi_c\left(-\frac{u}{\sqrt{1+u^2}}\right)du. \tag{7}$$

We finally propose the following substitution $v = u+\sqrt{1+u^2}$ which uniquely defines $u = \frac{v^2-1}{2v}$, and yields

$$L_m(x_a,x_b,\vec{\omega}) = I\frac{\kappa_s}{h}e^{\kappa_t(x_a-x_h)}2\int_{v_a}^{v_b}\frac{e^{-Hv}}{1+v^2}\Phi_c\left(\frac{1-v^2}{1+v^2}\right)dv \tag{8}$$

where we note $v_a = v(x_a)$ and $v_b = v(x_b)$ with

$$v(x) = \frac{x-x_h}{h}+\sqrt{1+\left(\frac{x-x_h}{h}\right)^2}. \tag{9}$$

While this formulation might still seem relatively convoluted, it is actually key to our approach and will allow the derivation of analytical solutions to the air-light integral as discussed in the subsequent sections.

3.3. Isotropic Phase Function

When considering an isotropic medium, the phase function reads $\Phi_c\left(\frac{1-v^2}{1+v^2}\right) = \frac{1}{4\pi}$ and equation 8 becomes

$$L_m(x_a,x_b,\vec{\omega}) = I\frac{\kappa_s}{h}e^{\kappa_t(x_a-x_h)}\frac{2}{4\pi}\int_{v_a}^{v_b}\frac{e^{-Hv}}{1+v^2}\,dv. \tag{10}$$

Defining the imaginary entity $\imath^2 = -1$ and Ei as the exponential integral function [AS72], the resulting integrand accepts an antiderivative known to be

$$\int\frac{e^{av}}{1+v^2}dv = \frac{\imath}{2}\left(e^{-\imath a}Ei(av+\imath a)-e^{\imath a}Ei(av-\imath a)\right). \tag{11}$$

Noting that $Ei(\bar{z}) = \overline{Ei(z)}$ and expanding each term into its real $\Re$ and imaginary $\Im$ parts, equation 11 simplifies into a function that we refer to as i_0 and which reads

$$\begin{aligned}\int\frac{e^{av}}{1+v^2}dv &= \sin(a)\Re(Ei(av+\imath a))-\cos(a)\Im(Ei(av+\imath a))\\ &= i_0(a,v).\end{aligned} \tag{12}$$

Defining $I_0(a,v_a,v_b) = i_0(a,v_b)-i_0(a,v_a)$, equation 10 can then be rewritten as follows

$$\begin{aligned}L_m(x_a,x_b,\vec{\omega}) &= I\frac{\kappa_s}{h}e^{\kappa_t(x_a-x_h)}\frac{2}{4\pi}I_0(-H,v_a,v_b)\\ &= I\frac{\kappa_s}{h}e^{\kappa_t(x_a-x_h)}\frac{2}{4\pi}\\ &\Big(\sin(-H)\Re\Big(Ei\big(-H(v_b+\imath)\big)-Ei\big(-H(v_a+\imath)\big)\Big)\\ &-\cos(-H)\Im\Big(Ei\big(-H(v_b+\imath)\big)-Ei\big(-H(v_a+\imath)\big)\Big)\Big).\end{aligned} \tag{13}$$

To the best of our knowledge, this is the first closed-form solution expressed in terms of well-known functions proposed in the literature to the air-light integral under the given assumptions. Although the solution involves a non-elementary special function, namely the exponential integral, it demonstrates the theoretical foundations for how the air-light integral relates to this standard mathematical entity.

3.4. Anisotropic Phase Function

We now show how the previous results can be extended to anisotropic media. Since deriving a custom analytical solution for all existing phase functions is obviously impossible, we seek a generic mechanism for them to expose a common interface. For this, we propose to use an expansion into a Taylor series as to express any phase function as a polynomial. Please note that unlike Lecocq's approach [LMAK00] where the entire integrand is expanded via an often arduous process into a series in order to easily approximate the integral, we only expand the phase function formulation as to provide a common generic representation. Doing so yields $\Phi_c\left(\frac{1-v^2}{1+v^2}\right) = \sum_{n=0}^{N-1}c_n v^n$ and equation 8 then becomes

$$L_m(x_a,x_b,\vec{\omega}) = I\frac{\kappa_s}{h}e^{\kappa_t(x_a-x_h)}2\sum_{n=0}^{N-1}c_n\int_{v_a}^{v_b}\frac{e^{-Hv}}{1+v^2}v^n\,dv. \tag{14}$$

As an antiderivative for the resulting integrand did not appear in any of the standard tables of integrals we had access to, we derived a generic solution on our own and verified the formulations obtained with this potentially new result for various individual values of n against the outputs provided by Mathematica. This solution reads

$$\int \frac{e^{av}}{1+v^2} v^n dv = e^{av} \sum_{j=0}^{n-2} v^j c(a,j,n) + \frac{1}{2}\left(\frac{1}{\imath^{n-1}} e^{-\imath a} Ei(av+\imath a) + \imath^{n-1} e^{\imath a} Ei(av-\imath a)\right) \quad (15)$$

where

$$c(a,j,n) = \sum_{\substack{i=(n-2-j) \bmod 2 \\ i+=2}}^{n-2-j} (-1)^{\frac{n-i-j}{2}} \frac{(i+j)!}{j!} \left(-\frac{1}{a}\right)^{i+1} \quad (16)$$

In order to express formula 15 in terms of real entities, we introduce the following antiderivative

$$\begin{aligned}\int \frac{e^{av}}{1+v^2} v dv &= \frac{1}{2}\left(e^{-\imath a} Ei(av+\imath a) + e^{\imath a} Ei(av-\imath a)\right) \\ &= \cos(a)\Re(Ei(av+\imath a)) + \sin(a)\Im(Ei(av+\imath a)) \\ &= i_1(a,v). \end{aligned} \quad (17)$$

Exploiting the periodicity of $\imath^{n-1}$ and expanding each term into its real and imaginary parts, it then follows that

$$\int \frac{e^{av}}{1+v^2} v^n dv = e^{av} \sum_{j=0}^{n-2} v^j c(a,j,n) + (-1)^{\lfloor \frac{n \bmod 4}{2} \rfloor} i_{(n \bmod 2)}(a,v). \quad (18)$$

Defining $I_1(a,v_a,v_b) = i_1(a,v_b) - i_1(a,v_a)$, the solution to equation 14 finally reads

$$L_m(x_a,x_b,\vec{\omega}) = I\frac{\kappa_s}{h} e^{\kappa_t(x_a-x_h)} 2 \sum_{n=0}^{N-1} c_n \left(\sum_{j=0}^{n-2}\left(e^{-Hv_b} v_b^j - e^{-Hv_a} v_a^j\right) c(-H,j,n) + (-1)^{\lfloor \frac{n \bmod 4}{2} \rfloor} I_{(n \bmod 2)}(-H,v_a,v_b)\right). \quad (19)$$

4. Implementation

Although several libraries provide implementations of the exponential integral, the latter belongs to the class of non-elementary special functions and is not part of the standard $C/C++$ libraries. Therefore, we chose to implement a custom solution optimized for the application of concern by amortizing computational efforts in a single iterative loop.

The exponential integral is most often evaluated via the following convergent series assuming $z \notin \{-\infty, 0\}$

$$Ei(z) = \gamma + \ln(z) + \sum_{k=1}^{\infty} \frac{z^k}{k\,k!} \quad (20)$$

where the Euler-Mascheroni constant is defined as $\gamma \approx 0.57721566490153286060651 2\ldots$ [AS72]. Formulating a complex number $z = x + \imath y$ into its exponential form $z = \rho e^{\imath\varphi}$ where $\rho = |z| = \sqrt{x^2+y^2}$ and $\varphi = Arg(z) = \text{atan2}(y,x)$ gives

$$\Re(Ei(z)) = \gamma + \ln(\rho) + \sum_{k=1}^{\infty} \frac{\rho^k}{k\,k!}\cos(k\varphi) \quad (21)$$

$$\Im(Ei(z)) = \varphi + \sum_{k=1}^{\infty} \frac{\rho^k}{k\,k!}\sin(k\varphi). \quad (22)$$

Defining $z_v = av + \imath a = \rho_v e^{\imath\varphi_v}$ where $\rho_v = \sqrt{a^2(v^2+1)}$ and $\varphi_v = \text{atan2}(a, av)$, equations 12 and 17 become

$$i_0(a,v) = \sin(a)(\gamma + \ln(\rho_v)) - \cos(a)\varphi_v + \sum_{k=1}^{\infty} \frac{\rho_v^k}{k\,k!}\sin(a-k\varphi_v) \quad (23)$$

$$i_1(a,v) = \cos(a)(\gamma + \ln(\rho_v)) + \sin(a)\varphi_v + \sum_{k=1}^{\infty} \frac{\rho_v^k}{k\,k!}\cos(a-k\varphi_v) \quad (24)$$

from which follows that

$$I_0(a,v_a,v_b) = \sin(a)\ln\left(\frac{\rho_{v_b}}{\rho_{v_a}}\right) - \cos(a)(\varphi_{v_b} - \varphi_{v_a}) + \sum_{k=1}^{\infty} \frac{1}{k\,k!}\left(\rho_{v_b}^k \sin(a-k\varphi_{v_b}) - \rho_{v_a}^k \sin(a-k\varphi_{v_a})\right) \quad (25)$$

$$I_1(a,v_a,v_b) = \cos(a)\ln\left(\frac{\rho_{v_b}}{\rho_{v_a}}\right) + \sin(a)(\varphi_{v_b} - \varphi_{v_a}) + \sum_{k=1}^{\infty} \frac{1}{k\,k!}\left(\rho_{v_b}^k \cos(a-k\varphi_{v_b}) - \rho_{v_a}^k \cos(a-k\varphi_{v_a})\right). \quad (26)$$

To exploit the similarities between the formulations of I_0 and I_1, we implemented a single function computing both results simultaneously and of which pseudo-code is provided in figure 2. The quality of the results is determined by line 25. interrupting the iterative process if the convergence test is satisfied. As the sine and cosine terms in the increments might reach local minima and provide an erroneous indication of the actual state of convergence, the test is performed on a distinct indicator being a conservative estimate of the potential amplitude of the increments obtained when the two terms have opposite signs. Depending on the needs, the indicator might be directly compared against the desired precision to provide a control on the absolute error or its product with each integral for a control on the relative error. Also, it is worth noting that the terms I_0 and I_1 in equation 19 are independent of the value of the iterator n and can consequently be computed once only before entering the loop.

5. Results

The method was implemented in a software ray-tracer running on an Intel Xeon 3.00GHz processor desktop. Performance characteristics for the various scenes are provided in table 1. In order to evaluate the quality of the results

1. **I01(a, va, vb, precision, maxIterations)**
2. $\rho_{v_a} = \text{sqrt}(a*a*(v_a*v_a+1))$;
3. $\rho_{v_b} = \text{sqrt}(a*a*(v_b*v_b+1))$;
4. $\varphi_{v_a} = \text{atan2}(a, a*v_a)$;
5. $\varphi_{v_b} = \text{atan2}(a, a*v_b)$;
6. $sin_a = \sin(a)$;
7. $cos_a = \cos(a)$;
8. $log_v = \log(\rho_{v_b}/\rho_{v_a})$;
9. $phi_v = \varphi_{v_b} - \varphi_{v_a}$;
10. $I_0 = sin_a * log_v - cos_a * phi_v$;
11. $I_1 = cos_a * log_v + sin_a * phi_v$;
12. $kfac = 1$;
13. $\rho^k_{v_a} = 1$;
14. $\rho^k_{v_b} = 1$;
15. $for(k = 1; k \leq maxIterations; k++)$
16. $\quad kfac* = k$;
17. $\quad \rho^k_{v_a}* = \rho_{v_a}$;
18. $\quad \rho^k_{v_b}* = \rho_{v_b}$;
19. $\quad \varphi_{kv_a} = a - k*\varphi_{v_a}$;
20. $\quad \varphi_{kv_b} = a - k*\varphi_{v_b}$;
21. $\quad denom = 1/(k*kfac)$;
22. $\quad I_0 += (\rho^k_{v_b} * \sin(\varphi_{kv_b}) - \rho^k_{v_a} * \sin(\varphi_{kv_a})) * denom$;
23. $\quad I_1 += (\rho^k_{v_b} * \cos(\varphi_{kv_b}) - \rho^k_{v_a} * \cos(\varphi_{kv_a})) * denom$;
24. $\quad indicator = (\rho^k_{v_b} + \rho^k_{v_a}) * denom$;
25. $\quad if(Converged(indicator, precision, I_0, I_1))break$;
26. $return(I_0, I_1)$;

Figure 2: *Pseudo-code of the function simultaneously computing $I_0(a, v_a, v_b)$ and $I_1(a, v_a, v_b)$*

over a wide range of ray trajectories, we experimented with an environment camera as shown in figure 3. When using Lecocq's method with the first 5 terms of the Taylor expansion as provided in [BMA03], ghosting artifacts occur in directions opposite to the light sources where negative estimates are generated followed by large over-evaluations. While the artifacts are less dramatic when bi-linearly interpolating Sun's 512x512 precomputed table made available by the authors, white spots remain due to the inability of the tabulated data to capture fine variations of the function. Moreover, inaccuracies occur in places where the distance parameter falls outside of the range of values handled by their table causing an erroneous brightening mostly visible under the arcades. On the other hand, our method automatically adapts to the required accuracy as to faithfully match the reference image. The quality of the results is highlighted in figure 6 where the errors here visible in our results are actually due to noise yet remaining in the reference solutions.

Figure 4 shows a scene containing an isotropic fog in which the air-light integral is evaluated independently for each color channel. When adjusting the step size as to match the rendering time of our approach, ray-marching yields severe undersampling artifacts. While being less obvious than previously, Lecocq's method also induces inaccuracies most noticeable around the glows of the light sources.

Figure	3 (1024x512)		4 (512x512)		5 (512x512)	
Metric	Time	Error	Time	Error	Time	Error
Ray-Marching			35 s	4.2e-2		
Lecocq	172 s	3.7e-2	29 s	3.6e-3	91 s	2.2e-2
Sun	168 s	3.4e-3				
Our Method	189 s	1.9e-4	35 s	5.5e-4	98 s	3.5e-3
Our Method 6					100 s	3.2e-4
Iterations	15.944628		6.053324		10.951751	

Table 1: *Performance characteristics for the various scenes rendered at the given resolution with 4 antialiasing samples per pixel, including rendering time and average error for ray-marching, Lecocq's method, Sun's method, and our analytical solution (with 3 and 6 coefficients for anisotropic media) along with the average number of iterations it required to reach an accuracy of 0.1%. Reference solutions were computed using Monte Carlo integration in 48 hours.*

Finally, figure 5 illustrates the results obtained for a Rayleigh phase function. In such anisotropic medium, Sun's approach is not practical as it requires a table to be precomputed for each possible value of the parameters of each possible phase function. Using only the first 3 terms of the Taylor expansion as reported by Biri et al. [BAM06], Lecocq's method leads to inaccuracies in the glow and to an erroneous darkening of the left side of the image while with the same number of terms, our approach matches the reference solution more closely. Also, the formulation of the terms used in a Taylor expansion typically requires a cascading derivation of the derivatives, generally through human intervention. In Lecocq's formulation, this process here becomes fairly intractable beyond the first 3 terms. Because our method relies on the expansion of the phase function only rather than the entire integrand, additional terms could be easily derived yielding results that here become virtually indistinguishable from the reference solution as shown in figure 6.

6. Discussion and Future Work

Besides its obvious coupling with a shadow volume algorithm as to naturally limit the integration domain to non-occluded ray segments, thus allowing the rendering of light shafts caused by the geometry as in [BAM06], we believe that our method could be improved in several ways.

While we demonstrated the potential of the technique for accuracy, we acknowledge that formulating the phase function in terms of a Taylor expansion might lead to precision issues, and further investigation is required to alleviate this limitation. Moreover, the extension to anisotropic light sources could be addressed as to make the method suitable to a broader spectrum of applications.

Regarding performance, while integration bounds distant from the light source might moderately affect the convergence rate of the solution, the latter will be more prominently

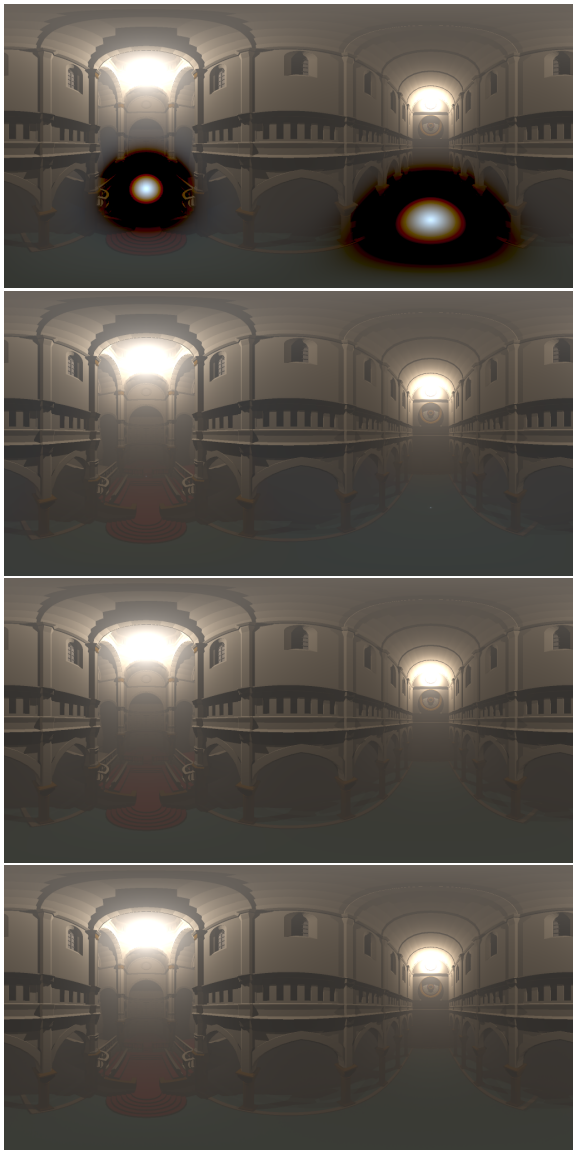

Figure 3: *The Sibenik cathedral filled with isotropic dust and illuminated by two white sources, rendered using (from top to bottom) Lecocq's method, Sun's method, our analytical approach, and Monte Carlo integration.*

impacted by the value of H. Therefore, the computational cost will increase as rays get farther away from the light, or in optically thick media but where the single-scattering assumption gets violated in the first place.

Also, the many more relatively expensive iterations required by our technique to achieve high quality results obviously entail a higher cost than Lecocq's approximation [LMAK00] or Sun's table look-up [SRNN05] as illustrated in the previous section. Furthermore, the reported timings

Figure 4: *A bridge by a foggy night illuminated by two colorful streetlamps, rendered using (top-left) ray-marching, (top-right) Lecocq's method, (bottom-left) our analytical approach, and (bottom-right) Monte Carlo integration.*

are probably not representative of the relative performance that would result from a GPU implementation and the aforementioned techniques are likely to be more adequate whenever real-time performance prevails over accuracy. Note however that the parameters of the integral in equation 8 can be trivially expressed in terms of an angular-distance coordinate pair (ϕ, H) via the relationship $u = \tan\left(\phi - \frac{\pi}{2}\right)$, and that the proposed solution is therefore readily applicable in place of numerical integration for efficiently precomputing Sun's 2D table. Nevertheless, we hope that mathematical advances on the study of special functions will allow the technique in itself to become more suitable to interactive applications in the near future, and have already shown its benefits over traditional ray-marching approaches.

7. Conclusion

In this paper, we have presented a novel analytical approach to single scattering from point light sources in homogeneous media. We have shown how to derive what we believe to be the very first closed-form solution expressed in terms of well-known functions to the air-light integral in isotropic media under the given assumptions, and discussed how this solution can be extended to anisotropic phase functions.

The technique relies neither on pre-computation nor on storage, and we have provided a practical implementation allowing for an explicit control on the precision of the solution, consequently yielding more accurate results than previous numerical and analytical methods as demonstrated both

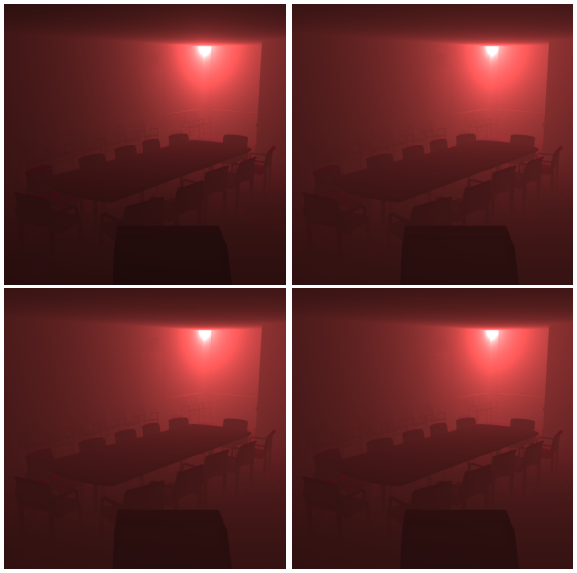

Figure 5: *The conference room filled with anisotropic smoke illuminated by an emergency light, rendered using (top-left) Lecocq's method with 3 terms, (top-right) our analytical approach with 3 terms, (bottom-left) our analytical approach with 6 terms, and (bottom-right) Monte Carlo integration.*

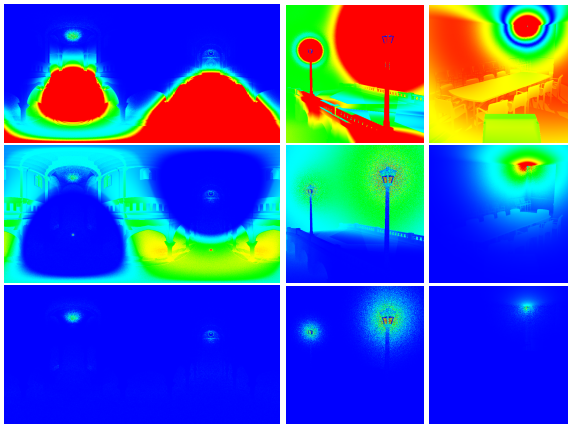

Figure 6: *Visualization of the absolute error mapped to hue (from blue to red) of the results (left) from figure 3 for (from top to bottom) Lecocq's method, Sun's method, and our analytical approach, (middle) from figure 4 for ray-marching, Lecocq's method, and our analytical approach, and (right) from figure 5 for Lecocq's method with 3 terms, and our analytical approach with 3 and 6 terms respectively.*

quantitatively and qualitatively. Although not readily suitable to real-time applications, we believe such type of analytical approach to be a promising alternative to traditional ray-marching/slice-based volume rendering techniques, and hope it will inspire subsequent research in the field.

Acknowledgments

This research was supported by the U.S. Department of Energy through the Center for the Simulation of Accidental Fires and Explosions, under grant W-7405-ENG-48. Sibenik cathedral model courtesy of Marko Dabrovic at RNA Studios, bridge model courtesy of NVIDIA Corporation, and conference room model courtesy of Greg Ward at LBL.

References

[AS72] ABRAMOWITZ M., STEGUN I. A.: *Handbook of Mathematical Functions with Formulas, Graphs, and Mathematical Tables*. U.S. Department of Commerce, 1972.

[BAM06] BIRI V., ARQUÈS D., MICHELIN S.: Real Time Rendering of Atmospheric Scattering and Volumetric Shadows. *Journal of WSCG 14* (2006), 65–72.

[Bli82] BLINN J. F.: Light Reflection Functions for Simulation of Clouds and Dusty Surfaces. *SIGGRAPH Computer Graphics 16*, 3 (1982), 21–29.

[BMA03] BIRI V., MICHELIN S., ARQUÈS D.: Real-Time Single Scattering with Shadows, 2003.

[CPCP*05] CEREZO E., PEREZ-CAZORLA F., PUEYO X., SERON F., SILLION F.: A Survey on Participating Media Rendering Techniques. *The Visual Computer 21*, 5 (2005), 303–328.

[DYN00] DOBASHI Y., YAMAMOTO T., NISHITA T.: Interactive Rendering Method for Displaying Shafts of Light. In *Pacific Graphics* (2000), pp. 31–37.

[DYN02] DOBASHI Y., YAMAMOTO T., NISHITA T.: Interactive Rendering of Atmospheric Scattering Effects Using Graphics Hardware. In *Graphics Hardware* (2002), pp. 99–107.

[ET08] E. M., T. S.: Volume Light. NVIDIA White Paper, 2008.

[HP02] HOFFMAN N., PREETHAM A. J.: Rendering Outdoor Light Scattering in Real Time. ATI White Paper, 2002.

[IJTN07] IMAGIRE T., JOHAN H., TAMURA N., NISHITA T.: Anti-Aliased and Real-Time Rendering of Scenes with Light Scattering Effects. *Visual Computer 23*, 9 (2007), 935–944.

[LMAK00] LECOCQ P., MICHELIN S., ARQUÈS D., KEMENY A.: Mathematical Approximation for Real-Time Lighting Rendering Through Participating Media. In *Pacific Graphics* (2000), pp. 400–401.

[Max86] MAX N. L.: Atmospheric Illumination and Shadows. *SIGGRAPH 20*, 4 (1986), 117–124.

[Mit07] MITCHELL K.: *GPU Gems 3*. 2007, ch. 13, pp. 275–285.

[NMN87] NISHITA T., MIYAWAKI Y., NAKAMAE E.: A Shading Model for Atmospheric Scattering Considering Luminous Intensity Distribution of Light Sources. *SIGGRAPH Computer Graphics 21*, 4 (1987), 303–310.

[REK*04] RILEY K., EBERT D. S., KRAUS M., TESSENDORF J., HANSEN C. D.: Efficient Rendering of Atmospheric Phenomena. In *Eurographics Symposium on Rendering* (2004), pp. 374–386.

[SH81] SIEGEL R., HOWELL J. R.: *Thermal Radiation Heat Transfer*. Hemisphere Publishing Corporation, 1981.

[SRNN05] SUN B., RAMAMOORTHI R., NARASIMHAN S. G., NAYAR S. K.: A Practical Analytic Single Scattering Model for Real Time Rendering. *Transactions on Graphics 24*, 3 (2005), 1040–1049.

[WR08] WYMAN C., RAMSEY S.: Interactive Volumetric Shadows in Participating Media with Single-Scattering. In *Symposium on Interactive Ray Tracing* (2008), pp. 87–92.